2011 American Control Conference
on O'Farrell Street, San Francisco, CA, USA
June 29 - July 01, 2011

Modeling and PI-Fuzzy logic controller of the Pierburg mechatronic actuator

A. Kebairi, M. Becherif and M. El Bagdouri

Abstract— **This paper focuses on the modeling, identification and control of the Pierburg mechatronic actuator. This is an air inlet swirl actuator. It is used in the BMW 6 cylinder diesel engine to control the air amount entering in the piston chamber. Physical model, which accurately reproduces the real behavior of this actuator, is developed using its static characteristics. This mechatronic actuator is subject of parameter variation during its life span. Therefore, a PI-Fuzzy logic controller is designed to ensure the desired performance. Simulation results using Simulink and experimental results using Labview with CompactRIO are presented. Results show that the PI-Fuzzy logic controller is able to govern the system and to guarantee the desired performance.**

I. INTRODUCTION

Mechatronics is a multidisciplinary engineering that aims to design simple, more efficient and reliable systems by combining the knowledge of numerous disciplines, such as the mechanics, the electronics, the control engineering, etc. Because of the development of these disciplines, mechatronics are becoming more and more important. Nowadays, the mechatronic systems are increasingly adopted to realize extremely important tasks and to accomplish very crucial actions. In motorization field, the mechatronic systems or also the mechatronic actuators are extensively used to improve the vehicle comfort as well as the engine efficiency. An important evolution of the internal combustion engine has been made using the mechatronic actuators to control its air path. As example, excellent air-fuel mixture implies high engine power production and low engine greenhouse gas emission. This may be achieved using inlet swirl actuators [21] to control the air amount entering into the cylinder, and exhaust gas recirculation actuators [22] to reduce the NO_x emission in internal combustion engines.

The Pierburg actuator is an electromechanical inlet swirl actuator. It is used in the BMW 6 cylinder diesel engine to control the air flow entering into the combustion chamber. Such system has a highly nonlinear behavior, due in part to external factors (temperature transients, disturbance...), and in other part to its own structure (gear systems relating the motor to the output shaft [1], springs [3], etc). Actually, such structure gives rise to extremely nonlinear phenomena such as friction forces, backlash phenomenon, hysteresis, etc. Therefore, the modeling of such system brings together knowledge of several disciplines such as: machine design [2], mechanic aspects [19], tribology [20], etc. Furthermore, the temperature transients and the material ageing cause parameter variations. Hence, an uncertain behavior is regenerated. Therefore, a robust controller is essential to ensure the desired performance while the system uncertainties occur. The fuzzy logic controller (FLC) has proven to be successful in the control of black box systems. It has also shown an improved performance over the classical controller when the transfer function is known [15]. Consequently, a lot of interest has been spent to the development and design of FLC, especially after the publication of L. A. Zadeh and E. H. Mamdani works [4], [5].

This paper addresses the modeling and identification of the Pierburg mechatronic actuator. Herein, the main objective is to design an appropriate model for simulation and control, a model which accurately reproduces the dynamics of the system taking in consideration the friction phenomenon. For this, the identification procedure given in [3], is applied. This procedure is based on the system's static characteristics. It allows, using standard techniques, to achieve the modeling objective mentioned above. Such system is subject of parameter variations, due to the ageing process and to some other external factors (e.g. temperature transients). Subsequently, a PI-fuzzy logic controller (PIFLC) is designed to ensure the desired performance even if the parameter variations occur. The effectiveness of the Pierburg simulator and the proposed controller are validated by simulation using Simulink and by experiments using Labview.

II. THE PIERBURG MECHATRONIC ACTUATOR

A. Actuator description

The Pierburg actuator is an inlet swirl actuator which is supposed to control the air amount entering in the piston chamber. Fig. 1-(A) illustrates the internal components of the considered system. While Fig. 1-(B) shows a simplified diagram of the actuator. Herein, two parts may be discerned: the electrical and the mechanical parts. The first one is a DC motor, whereas the second one includes a gear system and a helical spring attached to the output shaft. The electric motor is supplied by a pulse width modulated signal having a mean value that depends on the desired displacement. Then, the cogwheel mechanism transmits the mechanical power of the motor to the output shaft. This ranges from a minimum angle α_{min} of 0° to a maximum one α_{max} of 90°. The two limits α_{min} and α_{max} actually correspond on two mechanical stoppers ensuring the minimum and the maximum displacement. Within this interval, a Hall effect

This work was supported by the SIMBA national French project.

A. Kebairi is with SET, UTBM, Belfort, 90010, France; athmane.kebairi@utbm.fr

M. Becherif is with FEMTO-ST/FCLab, UMR CNRS 6174, UTBM, Belfort, 90010, France; mohamed.becherif@utbm.fr

M. El Bagdouri is with SET, UTBM, Belfort, 90010, France; mohammed.el-bagdouri@utbm.fr

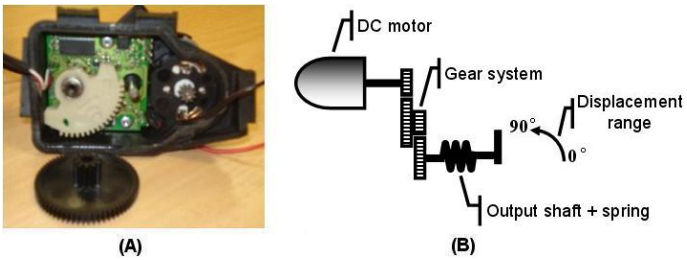

Fig. 1. The Pierburg actuator: (A) Internal components; (B) Simplified diagram.

sensor is used to determine the adjustment shaft position. Once the DC motor duty cycle is null, or in the case of electrical failure, the helical spring ensures the return of the adjustment shaft to the initial position α_{min}.

B. The Pierburg model

This section addresses the modeling of the system shown in Fig.1-(B). Herein, the entry of the system is the armature voltage whereas its output is the shaft displacement. Our objective is to design a model that accurately relates the armature voltage to the adjustment shaft position, taking into accounts the friction forces.

The electrical part of the Pierburg actuator is a standard DC motor. This may be described by the following linear equations:

$$\begin{aligned} U &= Ri + L\frac{di}{dt} + V_{emf} && (1)\\ T_m &= J\frac{d\omega_m}{dt} + f\omega_m + T_{load} && (2)\\ T_m &= k_m i \\ V_{emf} &= k_e \omega_m \end{aligned}$$

where U is the armature voltage. i, R and L are the motor current, resistance and inductance respectively. J is the motor inertia, f is the friction coefficient, ω_m is the motor velocity and T_{load} represents the load torque. V_{emf} and T_m are the back EMF and the motor torque, which are defined by the speed constant k_e and the torque constant k_m respectively.

The motor torque is transmitted to the output shaft by a gear system. This is supposed to be perfect (reducer). Therefore, its transmission coefficient may be given as:

$$k_g = \frac{\omega_m}{\omega} = \frac{T_{adj}}{T_m} \quad (3)$$

where T_{adj} and ω are the torque applying to, and the velocity of the output shaft respectively.

Applying the Newton's second law of motion to the output shaft gives:

$$\begin{aligned} J_t\frac{d\omega}{dt} &= T_{adj} - T_f - T_s - T_{Load}, && (4)\\ T_s &= k_s\theta + \Delta_s \end{aligned}$$

where J_t is the total inertia, T_{adj} is the torque applied to the adjustment shaft, T_f is the global friction torque, T_s is the spring torque, k_s is the spring elastic constant, Δ_s is a constant torque due to the pre-compression of the spring, and θ represents the adjustment shaft angle.

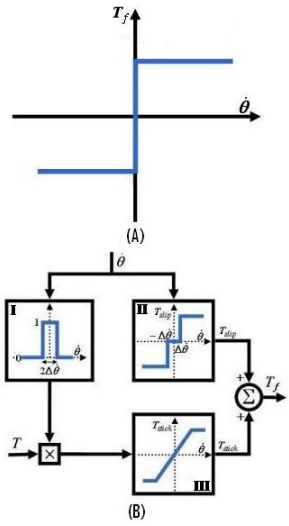

Fig. 2. Friction Force: (A) Coulomb friction model; (B) Karnopp model.

Assuming that:

- the torque and the speed constants are equals.
- the load torque T_{Load} is negligible [1].

And using (1), (3) and (4), the actuator dynamics may be described by the following equations:

$$\begin{aligned} U &= Ri + L\frac{di}{dt} + k_g k_m \frac{d\theta}{dt} && (5)\\ J_t\frac{d^2\theta}{dt^2} &= k_g k_m i - k_s\theta - \Delta_s - T_f && (6) \end{aligned}$$

C. The friction forces

Friction occurs in all systems including parts with relative motion. It is generally the force resisting to the relative motion of two surfaces in contact. As a rule, the friction causes degradations of system performance, and can generate limit cycles [12]. Therefore, study of the friction phenomenon is a pivotal step in modeling and control of machines or also electromechanical systems. In literature, numerous models have been proposed to reproduce the friction dynamics and to capture its characteristics [8], [9]. Fig. 2-(A) shows one of the simplest friction models. It only comprises one component,

[1] In the modeling and identification procedure, no load torque is applied

namely the Coulomb force which may be reproduced by a constant friction level acting in the direction opposite to motion. A crucial drawback of such model (generally, the classical friction models) is the discontinuity at zero velocity, which may lead to simulation difficulties. Such problem may be surmounted using either the dynamic friction models [10], [13], or one of the techniques given in [11], [14], [18]. In the following study, the Karnopp model will be used [11]. Fig. 2-(B) illustrates its block diagram. Herein, T, $\dot{\theta}$, T_{stick}, T_{slip} and T_f are the applied torque, the relative velocity, the static friction, the kinetic friction and the total friction force respectively. A small interval $[-\Delta\dot{\theta}, +\Delta\dot{\theta}]$ is defined where the velocity is forced to be zero. According to this, the friction force is calculated as follows:

- Velocity inside $[-\Delta\dot{\theta}, +\Delta\dot{\theta}]$: the friction is a function of the applied (external) torque. It is limited by the block III which is activated by the block I. Thus, the friction force may be mathematically expressed as follows:

$$T_{stick} = \begin{cases} T, & |T| < T_{stick.max} \\ T_{stick.max}, & Otherwise \end{cases} \quad (7)$$

- Velocity outside $[-\Delta\dot{\theta}, +\Delta\dot{\theta}]$: the friction is an instantaneous force-velocity curve, defined by the block II in Fig. 2-(B). Example for this is the Coulomb friction force:

$$T_{slip} = T_c sgn(\Delta\dot{\theta}) \quad (8)$$

The Karnopp model has been essentially developed to overcome the zero-velocity detection problem and to capture the stick-slip phenomenon, but it can also be used to regenerate the Coloumb model by fixing $T_{stick} = T_{slip}$.

D. Parameter identification

In order to identify the system parameters, we will use the procedure given in [3]. This method is based on the system static characteristics relating the DC motor duty cycle to the output shaft position. It allows to identify the Karnopp friction coefficients as well as the system parameters. In this study, it is assumed that:

- The friction forces may be simulated by the Coulomb model. Hence, the static friction and the viscous friction will be both neglected.
- The effect of the armature circuit current will be ignored.

Fig. 3 gives the theoretical static characteristics of the Pierburg actuator. Herein, D is the duty cycle, D_c and D_{pre} are the duty cycles required to overcome the Coulomb friction and the pre-compression torque respectively. Let V and U be the DC motor voltage supply and the armature voltage respectively. Then, the following expression is obtained:

$$U = DV, \quad D_c = \frac{T_{slip}R}{VK_gK_m}, \quad D_{pre} = \frac{\Delta_s R}{VK_gK_m}, \quad (9)$$

The values of D_c and D_{pre} can be determined by comparing the measured static characteristics to the theoritical curve given in Fig. 3. Once these two parameters are set, the

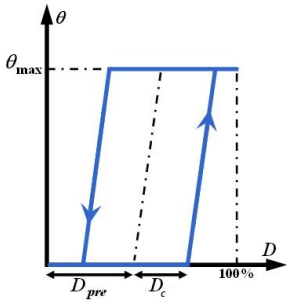

Fig. 3. Static characteristic of the Pierburg actuator.

duty cycle value D_m, which reproduces the movement of the mechatronic actuator, can be easily obtained as:

$$D_m = D - \frac{(T_{slip} + \Delta_s)R}{Vk_gk_m} \quad (10)$$

The system dynamics, which corresponds to the duty cycle value D_m, may be imitated by a 2^{nd} order linear system. Therefore, the other unknown parameters may be estimated by fitting the step response of the Pierburg actuator by the following expression:

$$\theta_s(t, p_i) = D_m VK(1 + \frac{p_2}{p_1 - p_2}exp(p_1 t) - \frac{p_1}{p_1 - p_2}exp(p_2 t)), \quad (11)$$

where

$$\begin{aligned} K &= \frac{k_g k_m}{Rk_s} \\ \omega_n^2 &= p_1 p_2 = \frac{k_s}{J_t} \\ \frac{2\xi}{\omega_n} &= \frac{p_1 + p_2}{p_1 p_2} = \frac{(k_m k_g)^2}{Rk_s} \end{aligned}$$

Here the damping ratio is considered to be greater than one, and $\theta_s(t, p_i)$ is the time evolution of the 2^{nd} order system for a step entry. ω_n is the system's natural pulse, ξ is the system's damping ratio, K and p_i are the unknown parameters representing the system gain and the system's poles respectively. These parameters can be estimated by solving the following least squares problem:

$$E = min \sum_{i=0}^{N} (\theta_s(t, p_i) - \theta)^2 \quad (12)$$

Where, E represents the error between the simulated displacement $\theta_s(t, p_i)$ and the real data θ. While N is the number of acquired samples.

TABLE I summarizes the system parameters that were calculated using (9)-(12). Herein, the gear ratio was provided by the constructor. The motor resistance can be directly measured when the output shaft is at a stationary position. These parameters were subsequently used to design a Pierburg actuator simulator in the Simulink environment. In Fig. 4, a comparison between the experimental data (continuous line) and the simulated data (dotted line) is given. From top to bottom, these curves show the system response for a step

TABLE I

THE IDENTIFICATION PARAMETERS.

Parameter	Signification
$K = 0.4363\ rad/volt$	The system gain
$\xi = 137.68$	The damping coefficient
$\omega_n = 240.16\ rad/sec$	The natural frequency
$R = 4.139\ \Omega$	The motor resistance
$k_g = 37.3$	The gear ratio
$k_s = 0.1419\ Nm/rad$	The elastic constant
$k_m = 0.022\ Nm/A$	The mechanical constant
$J_t = 2.460210^{-6}\ Kg.m^2$	The total inertia
$\Delta_s = 0.29\ Nm$	The pre-loading of the spring
$T_{slip} = 0.2007\ Nm$	The static and coulomb friction

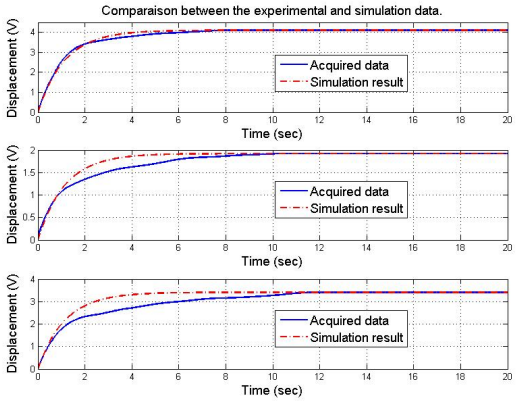

Fig. 4. Experimental and simulation results.

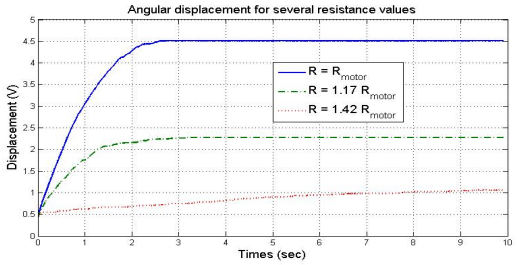

Fig. 5. Parameter variation effects.

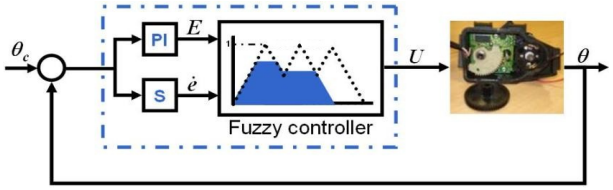

Fig. 6. The PI-Fuzzy controller.

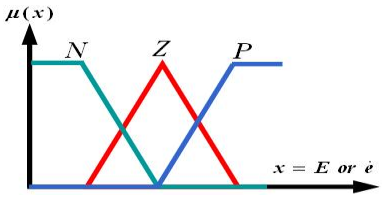

Fig. 7. Membership functions.

TABLE II

THE FUZZY LOGIC RULES.

		E		
		N	Z	P
$\dot{e}$	N	NB	N	Z
	Z	N	Z	P
	P	Z	P	PB

entry of $0 \mapsto 24\%$, $0 \mapsto 20\%$ and $0 \mapsto 22\%$ respectively. It can be seen that the simulation results corroborate well with the experimental data. The difference between the real and the simulated data can be justified by the fact that some phenomena, such as the backlash phenomenon, the static friction, the viscous friction, etc, were ignored.

III. A PI-FUZZY LOGIC CONTROL

Mathematical model, that can accurately reproduce the system dynamics and approximately predict the effects of parameter variations, is necessary for the control design. However, the model developed in the previous section does not perfectly reproduce the actuator behavior nor incorporate the effect of the parameter variations. The parameter variations may affect both the dynamics and the static characteristics of systems. In Fig. 5, we show the effect of the armature resistance variation, by adding an external resistor in series, on the actuator output. Hence, a simple or reduced model may not be reliable under some conditions. Therefore, the design of a controller that is robust against the parameter uncertainties is essential to ensure the desired performance. In this study, The FLC will be used. This has shown an ability to successfully control processes, where the transfer function is undefined, and improved performance over the classical controller, where the transfer function is known [15]. Therefore, a lot of interest has been given to the development and application of fuzzy logic to control systems [16], [17]. Several structures of the hybrid PID-fuzzy logic controller have been also proposed, as example, a self tuning fuzzy PID type controller was proposed in [6]. While in [7], a fuzzy logic block is used to tuned on-line the gains of the conventional PID controller, based on the error, its derivative and fuzzy inference.

The designed control structure, used here, is shown schematically in Fig. 6. Herein, the FLC is governed by two entries which are the PI controller output and the derivative of the error $\dot{e}$ respectively. According to these, the PIFLC regenerates the control signal U which is subsequently applied to the actuator in order to get the desired position. The controller signal U is determined basing on a set of fuzzy rules of the form:

$$\text{if the PI output is } A_i \text{ and } \dot{e} \text{ is } B_i, \text{ then } U \text{ is } C_i \quad i = 1,2,...,m. \tag{13}$$

Here, A_i, B_i and C_i are fuzzy sets on the corresponding sets. Table II gives the fuzzy logic rules used to evaluate the control signal. Herein, the abbreviations PB, P, Z, N and NB

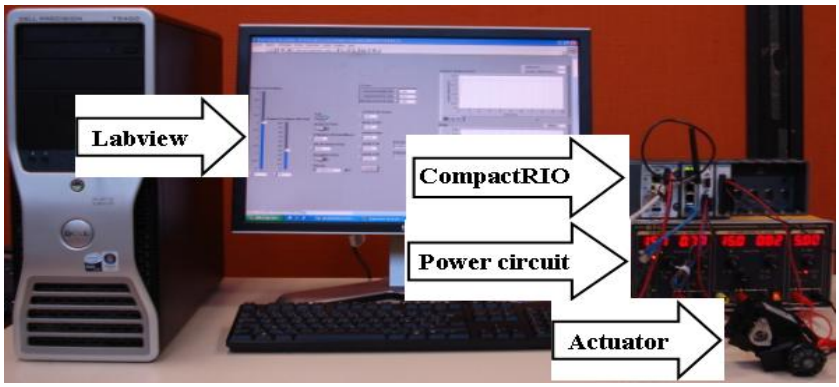

Fig. 8. The main hardware.

Fig. 9. System response for $R_{total} = R_{motor}$.

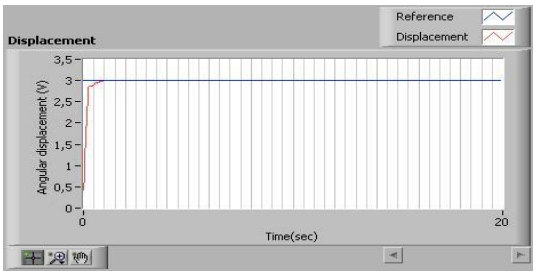

Fig. 11. System response for $R_{total} = 1.42R_{motor}$.

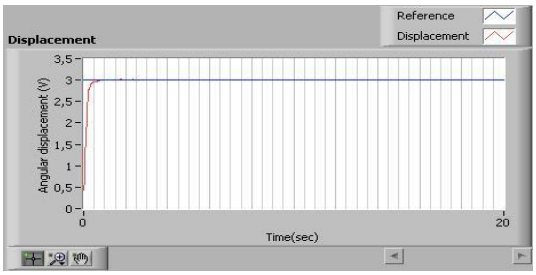

Fig. 10. System response for $R_{total} = 1.17R_{motor}$.

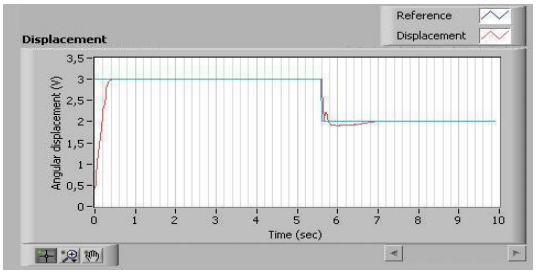

Fig. 12. Output for a square signal.

represent positive big, positive, zero, negative and negative big respectively.

Adding the proportional integral block in the controller simplifies building up the appropriate membership functions. In this work, it has been seen that using the standard triangular membership functions is sufficient to reach the desired closed-loop performance. Fig. 7 shows the set of membership functions used for both the PI output and the derivative of the error $\dot{e}$. The only difference between these two sets is the support interval, which is chosen according to the variation interval of the parameter, for example, the output displacement of the Pierburg actuator ranges from $0.42V$ $(0°)$ to $4.52V$ $(90°)$. Hence, the error is inevitably inside $[-4.1V, 4.1V]$. Therefore, the variation range of the PI output may be evaluated according to the PI gains. In the same way, the variation interval of $\dot{e}$ may be also estimated.

In order to test the controller performance, the PIFLC described in the previous section was implemented in the Labview environment. Hence, two programs were made. The first one is compiled in a field programmable gate array circuit (FPGA), which provides more accuracy and reliability. This one ensures the data transmission between the mechatronic actuator and the Labview software. Whereas, the second program is the Real-Time controller including the PIFLC program and some blocks to read from and write in the FPGA program. Fig. 8 shows the main hardware used to realize the experimentation. It consists of one CompactRIO NI cRIO-9022 (equipped by two modules: the NI 9215 A/D converter and the NI 9505 PWM generation), the Pierburg actuator, a power circuit and a computer. According to the PI output and the time derivative of the error, the PIFLC evaluates the control value. Then, the NI 9505 module re-generates the voltage amplitude corresponding to this value. Subsequently, the angular displacement is measured by a Hall effect sensor and acquired by the NI 9215 A/D converter module to be used in calculating the posterior error value,

and so on.

Fig.9-11 illustrate the experimental actuator behavior for a total resistance $R_T = R_{motor}$, $R_T = 1.17R_{motor}$ and $R_T = 1.42R_{motor}$ respectively. These results show that the PIFLC is robust against the parameter uncertainties and it is able to ensure the desired displacement. The realized tests show that the actuator response changes according to the PI gains and the displacement direction. Fig.12 illustrates the system response for a square signal. When the angular displacement goes in the clockwise direction, the motor and the spring torque have the same direction, and generally, there is a small overshoot.

IV. Conclusion

In this paper, a global study of the Pierburg mechatronic actuator has been presented. First, a physical model that accurately makes the relationship between the armature voltage and the output shaft displacement has been developed using the Newton's and the Kirchhoff's laws. Next, the static characteristics of the system have been exploited to identify both the actuator parameters and the friction model coefficients. Then, a PIFLC was designed to achieve the desired performance even if the parameters variation occurs. Experimental results using Labview with CompactRIO and simulation results using Simulink have shown the effectiveness of both the actuator simulator and the performance and robustness of the PIFLC.

References

[1] J. B. Song and K. S. Byun, Throttle actuator control system for vehicle traction control, Mechatronics, Volume 9, Issue 5, Pages 477-495, 1999.

[2] J. Chiasson, Modeling and High-Performance Control of Electric Machines, IEEE Series on Power Engineering, NY: Wiley, 2005.

[3] R. Scattolini, C. Siviero, M. Mazzucco, S. Ricci, L. Poggio and C. Rossi, Modeling and identification of an electromechanical internal combustion engine throttle body, Control Engineering Practice, Volume 5, Issue 9, Pages 1253-1259, September 1997.

[4] L. A. Zadeh, Fuzzy sets, Information and Control, Volume 8, Pages 338-353, 1965.

[5] E. H. Mamdani, Application of fuzzy algorithms for control of simple dynamic plant, IEEE Proc, Volume 121, Issue 12, Pages 1585-1588, 1974.

[6] E. Yaşil, M. Güzelkaya and İ. Eksin, Self tuning fuzzy PID type load and frequency controller, Energy Conversion and Management, Volume 45, Pages 377-390, February 2004.

[7] Z. Y. Zhao, M. Tomizuka and S. Isaka, Fuzzy gain scheduling of PID controllers, IEEE Transactions on Systems, Man and Cybernetics, Volume 23, Issue 5, Pages 1392-1398, 1993.

[8] H. Olsson, K. J. Åström, C. Canudas DE Wit, M. Gäfvert, and P. Lischinsky, Friction models and friction compensation, European J. on Control, 1998.

[9] B. Borsotto, Modélisation, Identification et commande d'un organe de friction Application au contrôle d'un systéme d'embrayage et au filtrage d'acyclismes par glissement piloté, PhD thesis Supélec, Faculté Des Sciences D'Orsay, Université Paris-Sud 11, Paris, France, 2009.

[10] D. A. Haessig and B. Friedland, On the modelling and simulation of friction, J. Dyn. Sys., Meas., Control, Volume 113, Issue 3, Pages 354-362, September 1991.

[11] D. Karnopp, Computer simulation of stick-slip friction in mechanical dynamic systems, J. Dyn. Sys., Meas., Control, Volume 107, Issue 1, Pages 100-103, 1985.

[12] H. Olsson and K. J. Åström, Friction generated limit cycles, Proc IEEE International Conference on Control Applications, Pages 798-803, Dearborn, MI, USA, 1996.

[13] B. Armstrong and Q. Chen, The Z-properties chart, IEEE Control Systems Magazine, Volume 28, Issue 5, Pages 79-89, 2008.

[14] D. C. Threlfall, The inclusion of coulomb friction in mechanisms programs with particular reference to dram, Mechanism and Machine Theory, Volume 13, Issue 4, Pages 475-483, 1978.

[15] G. S. Sandhu, T. Brehm and K. S. Rattan, Analysis and design of a proportional plus derivative fuzzy logic controller, Proc IEEE aerospace and Electronics Conference, Volume 1, Pages 397-404, Dayton, OH, USA, 1996.

[16] C. C. Lee, Fuzzy logic in control systems: fuzzy logic controller. I, IEEE Transactions on Systems Man and Cybernetics, Volume 20, Issue 2, Pages 404-418, 1990.

[17] C. C. Lee, Fuzzy logic in control systems: fuzzy logic controller. II, IEEE Transactions on Systems Man and Cybernetics, Volume 20, Issue 2, Pages 419-435, 1990.

[18] F. Altpeter, Friction Modeling, Identification And Compensation, PhD thesis, Ecole Polytechnique Fédérale de Lausanne, 1999.

[19] C. K. Benjamin, Automatic Control Systems, 8th ed, Wiley, 2002.

[20] B. Armstrong-Hélouvry, P. Dupont and C. Canudas de Wit, A survey of models, analysis tools and compensation methods for the control of machines with friction, Automatica, Volume 30, Issue 7, Pages 1083-1138, 1994.

[21] A. Kebairi, S. CAI, M. Becherif, M. El-Bagdouri, Modeling and Passivity-Based Control of the Pierburg Mechatronic Actuator, Proc of Conference on Control and Fault Tolerant Systems, France, 2010.

[22] S. Laghrouche, F.S. Ahmed, M. El Bagdouri, M. Wack, J. Gaber and M. Becherif, Modeling and Identification of a Mechatronic Exhaust Gas Recirculation Actuator of an Internal Combustion Engine, Proc IEEE American Control Conference, Baltimore, MD, USA, Pages 2242-2247, 2010.